

A EUROPEAN JOURNAL OF CHEMICAL BIOLOGY

CHEM **BIO** CHEM

SYNTHETIC BIOLOGY & BIO-NANOTECHNOLOGY

Accepted Article

Title: Structural Insights into Conformational Differences between DNA/TNA and RNA/TNA Chimeric Duplexes

Authors: Irina Anosova; Ewa A. Kowal; Nicholas J. Sisco; Sujay Sau; Jen-Yu Liao; Saikat Bala; Eriks Rozners; Martin Egli; John C. Chaput; Wade D Van Horn

This manuscript has been accepted after peer review and the authors have elected to post their Accepted Article online prior to editing, proofing, and formal publication of the final Version of Record (VoR). This work is currently citable by using the Digital Object Identifier (DOI) given below. The VoR will be published online in Early View as soon as possible and may be different to this Accepted Article as a result of editing. Readers should obtain the VoR from the journal website shown below when it is published to ensure accuracy of information. The authors are responsible for the content of this Accepted Article.

To be cited as: ChemBioChem 10.1002/cbic.201600349

Link to VoR: <http://dx.doi.org/10.1002/cbic.201600349>

A Journal of



www.chembiochem.org

WILEY-VCH

Structural Insights into Conformational Differences between DNA/TNA and RNA/TNA Chimeric Duplexes

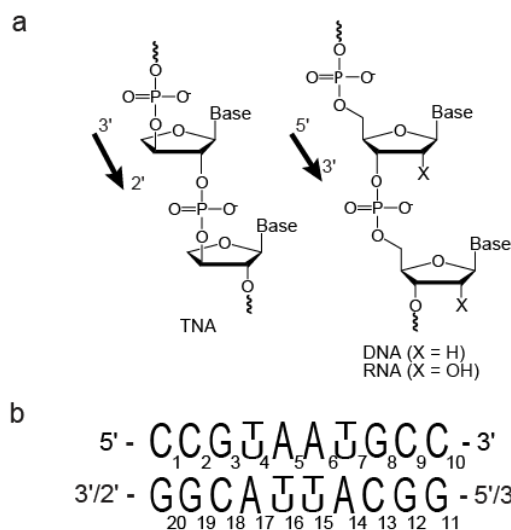
Irina Anosova, Ewa A. Kowal, Nicholas J. Sisco, Sujay Sau, Jen-yu Liao, Saikat Bala, Eriks Rozners, Martin Egli, John C. Chaput and Wade D. Van Horn*

Abstract: Threose nucleic acid (TNA) is an artificial genetic polymer capable of heredity and evolution that is studied in the context of RNA chemical etiology. Its simplified four-carbon threose backbone replaces the five-carbon ribose in natural nucleic acids. Nonetheless, TNA forms stable antiparallel Watson-Crick homoduplexes and heteroduplexes with complementary DNA and RNA. TNA base pairs with RNA more favorably than DNA, but the reason is unknown. Here, we employ NMR, ITC, UV and CD studies to probe the structural and dynamic properties of RNA/TNA and DNA/TNA heteroduplexes that give rise to the differential stability. The results indicate that TNA templates the structure of heteroduplexes, forcing an A-like helical geometry. Further NMR measurements of kinetic and thermodynamic parameters for individual base pair opening events reveal unexpected asymmetric breathing fluctuations of the DNA/TNA helix, which are also manifested at the molecular level. These results suggest that DNA is unable to fully adapt to the conformational constraints of the rigid TNA backbone and that nucleic acid breathing dynamics are determined from both backbone and base contributions.

TNA (α -L-(3'-2')-threofuranosyl nucleic acid) is an alternative genetic polymer in which the natural ribose sugar found in RNA has been replaced with an unnatural four-carbon sugar of α -L-threose (Scheme 1a).^[1] Despite a backbone repeat unit that is one atom shorter than that found in DNA and RNA, TNA is capable of adopting stable Watson-Crick duplex structures with itself and with complementary strands of DNA and RNA.^[1a, 2] The ability to exchange genetic information with RNA has raised significant interest in TNA as an RNA progenitor during the early stages of life on Earth.^[3]

Relative to natural DNA and RNA, TNA has a sugar-phosphate backbone composed of quasi *trans*-diaxial 3'-2' phosphodiester linkages, which places the phosphate groups in distinct relative positions.^[4] Crystallographic analysis of B- and A-form duplexes with a single TNA nucleotide inserted into an otherwise natural DNA strand yielded only minor effects on the duplex geometries, base-pair stacking interactions, and the sugar pucker of neighboring native nucleotides.^[5, 6] In both structures, the threose sugar adopts a C4'-exo-pucker with a *trans*-diaxial orientation of the 3'- and 2'-substituents. The preference for this sugar conformation,

irrespective of the A- or B-form geometry, suggests that TNA has a limited range of sugar conformations that are compati-



ble with Watson-Crick base pairing.

Scheme 1. Backbone structure and nucleotide sequences of TNA, DNA, and RNA. (a) Constitutional structure of the linear backbone and strand directionality of TNA (left panel), and DNA/RNA (right panel). (b) Palindromic nucleotide sequences used in this study. For the chimeric duplexes, the bottom strand was composed of TNA.

Previous studies have shown that sequence can have dramatic effects on homo- and heteroduplex stability of both natural and artificial genetic polymers.^[7] As a result, in this study we focus on a single duplex sequence and examine the structural properties and Watson-Crick base pairing dynamics of a model palindromic decamer sequence (Scheme 1b) constructed as DNA/TNA and RNA/TNA heteroduplexes. The bottom strands of the chimeric duplexes are composed of TNA. The TNA strand was generated by solid-phase synthesis using chemically synthesized TNA phosphoramidites.^[8] Equivalent DNA and RNA homoduplexes were prepared and studied as a direct comparison to standard B- and A-form helices, respectively.

1D ¹H NMR spectra of the homo- and heteroduplexes indicate that all four helices form standard Watson-Crick interactions as identified from the chemical shift and dispersion of the imino proton resonances (12–14 ppm, Figure S1). At low temperature, each decamer has eight sharp imino proton resonances, representative of stable duplexes with fraying exclusively at the terminal bases. Imino proton NMR spectra of the DNA and RNA helices between 5 and 50 °C (Figure S2) indicate that the DNA structures have lower thermal stability than the RNA structures. Consistent with the NMR data, UV spectroscopy thermal denaturation curves yielded melting temperature (T_m) values that are ~10 °C lower for the DNA/TNA and DNA/DNA duplexes, compared to the RNA/TNA and the RNA/RNA duplexes, respectively (Figure 1a).

Thermal denaturation studies show that each chimeric duplex is similar in stability to its corresponding homoduplex

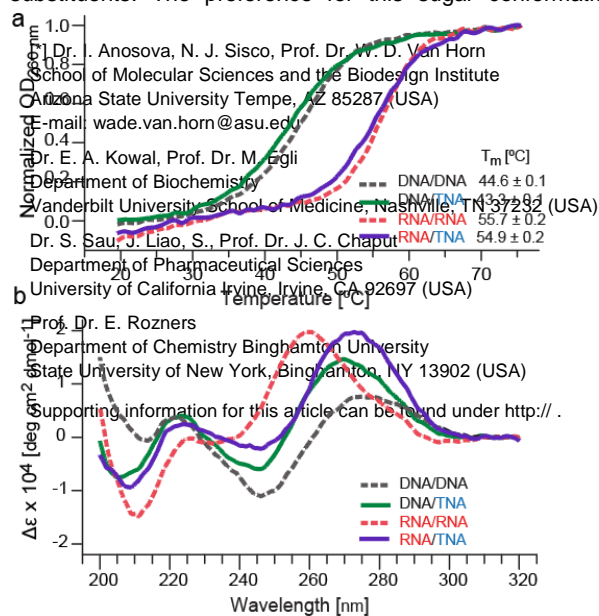


(Figure 1a). This observation is consistent with previous analyses performed on mixed-sequence TNA/RNA and TNA/DNA hetero- and homoduplexes.^[1a] Moreover, the T_m values observed by UV spectroscopy melting are partially reflected by the thermodynamic parameters obtained by isothermal titration calorimetry (ITC, Table 1, and Figure S3). The ITC results indicate that all duplexes have similar association stabilities with an average ΔG of -43 ± 3 kJ/mol. However, the dissociation constants (K_D) differ significantly between the duplexes (Table 1). While K_D values of the double stranded DNA (15 nM), RNA (12 nM) and RNA/TNA (45 nM) duplexes are all in the low nanomolar range, the K_D of the DNA/TNA heteroduplex is clearly higher (135 nM), suggesting that a modest degree of structural incompatibility or increased dynamics exists within DNA/TNA heteroduplex.

Figure 1. Thermal stability and CD analysis of model duplexes composed of DNA/TNA, DNA/DNA, RNA/TNA, and RNA/RNA. (a) Normalized UV-detected melting curves collected at 260 nm. T_m values for each curve are provided in the lower right corner. (b) CD spectra overlaid for each duplex acquired at pH 7.0 and 25 °C. Data are in units of mean residue molar ellipticity ($\Delta\epsilon$, deg cm² dmol⁻¹).

CD spectra also reveal the existence of conformational differences between the homo- and heteroduplexes (Figure 1b). As expected, the CD spectrum from DNA/DNA is typical of a standard B-form helix, with low mean residue molar ellipticity ($\Delta\epsilon$) arising from lower chirality of the perpendicularly oriented base pairs, a positive peak at 275 nm and a negative peak at 245 nm. The CD spectrum of RNA/RNA is consistent with an A-form helix with a positive peak at 260 nm and a negative peak near 210 nm. Compared to the natural duplexes, both the DNA/TNA and RNA/TNA heteroduplexes exhibit $\Delta\epsilon$ values comparable to double stranded RNA with maxima near 270 nm, minima at 245 nm, and strong negative bands near 210 nm, consistent with an A-form conformation and suggestive that TNA prefers an RNA-like helical form.

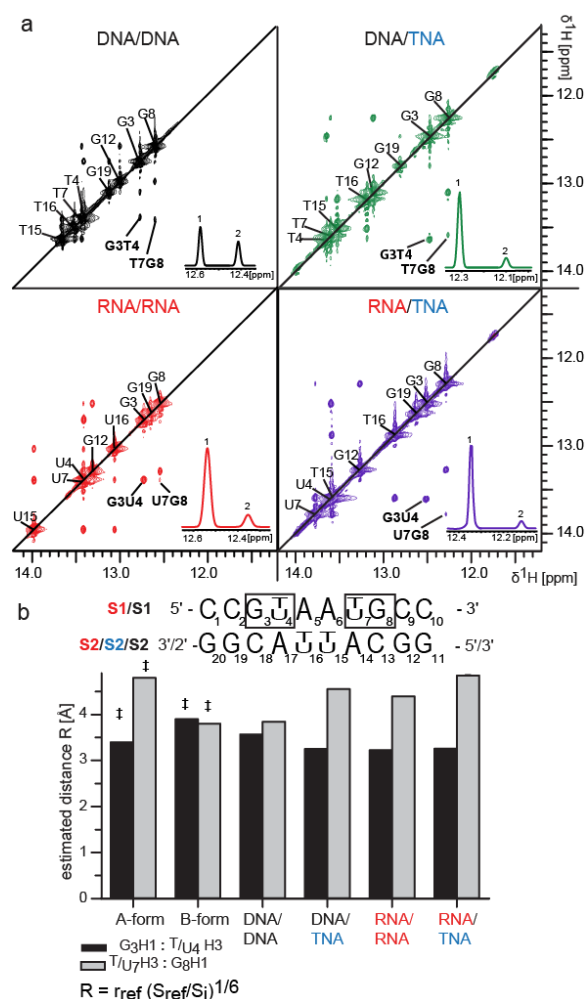
Table 1. Thermodynamic parameters from ITC.

	DNA/DNA	DNA/TNA	RNA/RNA	RNA/TNA
K_D [nM]	15.0 ± 3.0	134.5 ± 5.4	11.7 ± 3.0	45.0 ± 4.6
ΔH [kJ mol ⁻¹]	-278 ± 11	-258 ± 16	-330 ± 6	-240 ± 5
ΔG [kJ mol ⁻¹]	-44.8 ± 0.5	-39.3 ± 0.1	-45.4 ± 0.6	-42.0 ± 0.3
$-T\Delta S$ [kJ mol ⁻¹]	234 ± 11	219 ± 16	284 ± 6	198 ± 4

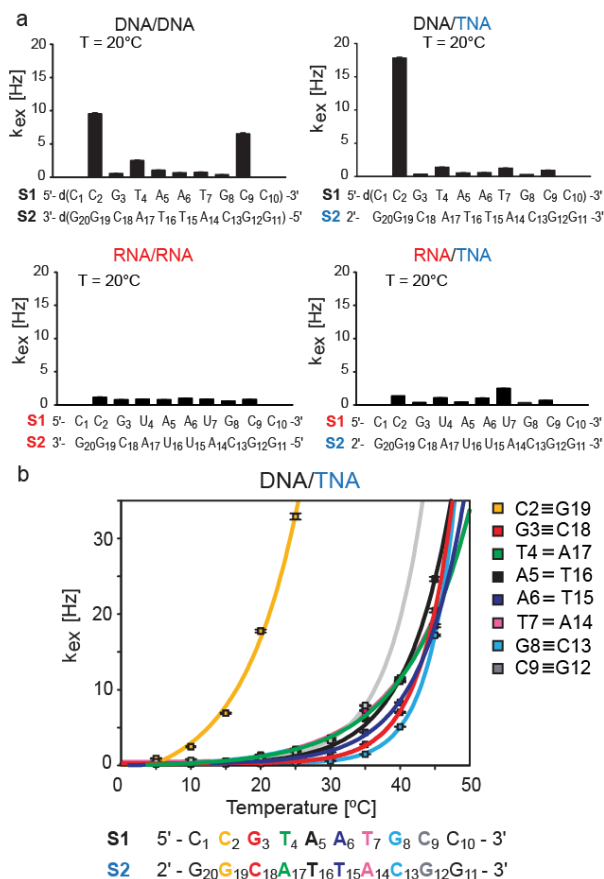
NMR-detected imino protons are very sensitive to nucleic acid secondary structure.^[9] To further evaluate the helical nature of TNA heteroduplexes, we recorded ¹H-¹H NOESY spectra for each construct in aqueous buffer at 15 °C and assigned the imino proton resonances (Figure 2a). As expected, imino protons for terminal base pairs of C1-G20 and

C10-G11 were not observed due to their rapid exchange with water. However, all other imino protons were clearly identified. Consistent with their respective helical geometries, standard A-form RNA and B-form DNA duplexes yield imino NOE cross-peaks with high and low peak intensities, respectively. In agreement with the CD analysis, the NMR imino regions of the RNA/TNA, and DNA/TNA duplex spectra are similar to the A-form RNA/RNA duplex (Figure 2a). This result is most easily observed by comparing the G3-T(U)4 and T(U)7-G8 NOESY cross peaks.

Figure 2. Conformational analysis of TNA heteroduplexes by solution NMR. (a) Imino regions of 1H-1H NOESY spectra of hetero- and homoduplexes measured at 15 °C. Spectra were scaled for comparison. Diagonal peaks are assigned with the diagonal shown as black line. Sequential peaks G3-T(U)4 and T(U)7-G8 used in quantitative analysis are indicated and their Gaussian-fitted direct dimension profiles are shown in the lower right corner of each panel with positions indicated by (1) and (2), respectively. (b) Top: generalized sequence of the studied duplexes with positions of the analyzed sequential bases being boxed. Bottom: estimated sequential 1H-1H distance (R) of G3H1:T(U)4H3 (gray bars) and T(U)7H3:G8H1 in 5'-3' direction in the studied constructs, as compared to standard values of canonical A- and B-form DNA (\ddagger). The strand identifiers are color coded according to the nucleic acid of origin.



Estimated sequential imino distances for the G3-T(U)4 and T(U)7-G8 bases in a 5'-3' direction were calculated from NOE cross-peak intensities under the initial rate approximation^[10] (see Supporting Information). As expected, the dis-



tances are consistent with the DNA/DNA duplex having a B-form helix. The RNA/RNA, RNA/TNA and DNA/TNA duplex distances are consistent with A-like helical geometries (Figure 2a).^[9] Taken together, these data indicate that TNA templates heteroduplex structures to form A-like helices.

Figure 3. Individual base pair stabilities of DNA and RNA homoduplexes and the corresponding TNA heteroduplexes. (a) Solvent exchange rates (k_{ex}) of imino protons in individual base pairs of DNA/DNA and DNA/TNA (top) compared to RNA/RNA and RNA/TNA (bottom) at 20 °C, depicted on top of the corresponding sequences. (b) Temperature dependence of imino proton solvent exchange rates (k_{ex}) for single base pairs in DNA/TNA. The corresponding fits of temperature-dependent k_{ex} data to Equation 6 in the Supporting Information are shown as solid lines that are color coded with the DNA/TNA duplex sequence below.

To better understand the stability and dynamics of the TNA heteroduplexes, we measured the rate of single base pair breathing events by NMR. Breathing motions in nucleic acid polymers are accompanied by the exchange of base imino hydrogens with water protons present in the aqueous surrounding.^[11] We measured and analyzed imino proton solvent exchange rate constants (k_{ex}) and estimated the individual base pair stability in each of the four duplexes using solvent-exchange-based NMR methods (Figures 3a and S4).^[12] The directionality of each duplex was assigned from ¹H-¹H NOESY anomeric-aromatic proton walks and directional H1'-H6/H8 correlations.^[13] Single base pair stability analysis was performed for base pairs C2-G19 through C9-G12. Terminal k_{ex} values were lower for RNA self-pairing and cross-pairing with TNA as compared to DNA self-pairing and cross-pairing with TNA (Figure 3a). Fraying of the bases in the RNA duplexes is limited to the terminal base pairs of C1-G20 and C10-G11 and the k_{ex} values are

uniformly low throughout the sequence with a slight increase in variability for the RNA/TNA duplex. With the exception of the penultimate base pairs, the DNA/DNA homoduplex also exhibits generally low flexibility in the core of the duplex structure with k_{ex} rates comparable to those observed for the RNA/RNA duplex. However, the penultimate base pair exchange rates rise symmetrically (~5-fold) over those observed in the core of the helix, consistent with symmetric, elevated motions at the duplex ends.

Base pair kinetics in the DNA/TNA heteroduplex revealed a previously uncharacterized asymmetric terminal exchange that is ~20-times faster k_{ex} (C2-G19) at the 5'/2' end of the helix than the rest of the helix, where k_{ex} values remained low and comparable to rates observed in the other constructs. Fraying at the 3'/3' end was again limited solely to the terminal base pair. Differences in the intramolecular dynamics of the DNA/DNA and DNA/TNA were also observed at the duplex level as differences in translational diffusion rates, measured by NMR, with the DNA/TNA diffusing slower (Figure S5). The strong terminal fraying of DNA/DNA and DNA/TNA may explain the observed differences in thermal stability between them and the RNA homoduplex and heteroduplex with TNA. Surprisingly the TNA/DNA duplex forms a dynamic, non-symmetric duplex structure in solution. The experiments were recorded at buffer concentrations that allow multiple closing and opening base-pair events prior to imino proton exchange (EX2 regime). This indicates that the asymmetric distribution of DNA/TNA k_{ex} values arise primarily from increased flexibility of the 5'/2' end of the DNA/TNA heteroduplex. The lack of one carbon per residue in the threose-linked strand presumably causes TNA to exhibit increased backbone rigidity relative to the natural ribose-based backbones. Our data suggests that unlike RNA, DNA may be facing the limits of its structural variability when paired with TNA. This hypothesis is rooted in the phosphate group pitch differences of DNA (~6.8 Å), RNA (~6.0 Å) and TNA (~5.7 Å) caused by the sugar pucker. The high entropic costs for pucker adaptation will increase with oligonucleotide length, potentially explaining the elevated K_D of the DNA/TNA duplex formation and limiting the duplex formation to relatively short polymers.

To investigate asymmetric base pair breathing in the DNA/TNA heteroduplex, we measured the individual base pair imino proton exchange rates as a function of temperature (Figure 3b).^[14] As expected, k_{ex} (C2-G19) increased with temperature until reaching a detection limit (asymptote) at 25 °C. By comparison, exchange rates of other base pairs followed a much slower temperature-dependent exponential curve, reaching their detection limits at ≥40 °C. By fitting the temperature dependent k_{ex} (see Supporting Information, Equation 6), we extracted the enthalpy (ΔH_{Diss}) and entropy (ΔS_{Diss}) of single base pair dissociations in the DNA/TNA duplex. The Gibbs free energy of the process (ΔG_{Diss}) was calculated according to the Gibbs-Helmholtz equation (Table 2).

Table 2. Thermodynamics of DNA/TNA duplex individual base pair openings^[a].

DNA/TNA ^[b]	ΔH_{Diss} [kJ mol ⁻¹]	ΔS_{Diss} [J mol ⁻¹ K ⁻¹]	ΔG_{Diss} [kJ mol ⁻¹] [T = 20°C]	T ΔS_{Diss} [kJ mol ⁻¹] [T = 20°C]
C2 ≡ G19	73 ± 8	198 ± 27	15 ± 11	58 ± 8
G3 ≡ C18	145 ± 3	396 ± 9	29 ± 4	116 ± 3
T4 = A17	42 ± 3	74 ± 10	20 ± 4	22 ± 3
A5 = T16	82 ± 5	201 ± 17	23 ± 7	59 ± 5
A6 = T15	84 ± 4	206 ± 12	24 ± 5	60 ± 3
T7 = A14	44 ± 4	80 ± 15	21 ± 7	23 ± 4
G8 ≡ C13	175 ± 1	490 ± 4	31 ± 2	144 ± 1

C9 = G12	112 ± 8	299 ± 27	24 ± 11	88 ± 8
----------	---------	----------	---------	--------

[a] Data were recorded at 20 °C. [b] TNA bases are colored blue.

The measured DNA/TNA heteroduplex thermodynamic values for single base-pair breathing events are similar to previously reported values from DNA and RNA duplexes, stem regions of RNA loops^[14], and imino exchange rates measured at elevated exchange catalyst concentrations.^[15] The magnitude and sign of ΔH_{Diss} suggest that the base pairs of DNA/TNA are enthalpically stabilized. Higher values at the ends for $\Delta H_{Diss}(GC)$ than $\Delta H_{Diss}(AT)$ in the middle of the sequence likely reflect the formation of all three hydrogen bonds between guanine and cytosine bases. Compared to ΔG_{Diss} reported for central bases in DNA duplexes (24 kJ/mol to 32.6 kJ/mol)^[14b, 15a] ΔG_{Diss} for DNA/TNA central pairs were mostly at the lower end of the range. The asymmetry of duplex breathing was reflected with a distribution of ΔG_{Diss} values. Central base pairs for the DNA/TNA helix showed comparable ΔG_{Diss} values; however, the ΔG_{Diss} (C2-G19) is consistent with the dynamic behavior and lower stability of the 5'-DNA/2'-TNA end.

In general, ΔG_{Diss} for each base pair was far less than the absolute value of ΔG for the heteroduplex formation detected by ITC, indicating that DNA/TNA heteroduplex stability is highly cooperative in nature. The distribution of ΔG_{Diss} values suggest that the opening of single DNA/TNA base pairs is primarily uncorrelated at 20 °C. Enthalpy-entropy compensation, i.e. the variations of ΔH_{Diss} and ΔS_{Diss} that offset one another to allow biologically accessible ΔG_{Diss} values, was observed for single base pairs in the DNA/TNA helix, suggesting that similar processes that underlie RNA duplex melting are involved in TNA-DNA heteroduplex stabilization. Historically, this effect was observed macroscopically across related systems^[16] and more recently was described at the single base pair level in a double stranded RNA stem.^[14a]

In summary, we report an extensive biophysical and thermodynamic characterization of base-pairing interactions between TNA and DNA and RNA. Our results show that despite similar thermal and thermodynamic stabilities TNA strongly favors an A-like helical geometry when base paired with either DNA or RNA. Thermodynamic characterization of single base pair opening events indicates that the enhanced stability of RNA/TNA base pairing over DNA/TNA base pairing is due to asymmetric fraying at the 5'/2' terminus of the DNA/TNA duplex. This previously uncharacterized effect manifests itself at the macromolecular level through distinct hydrodynamic differences between the DNA/TNA heteroduplex and the DNA homoduplex. We suggest that this phenomenon is likely due to an inability of DNA to fully adapt to the conformational constraints of a rigid TNA backbone. As a result, structural studies of DNA/TNA chimeric duplexes could prove challenging. These data also suggest that in

addition to thermodynamic differences in stability between AT- and GC-rich nucleic acid segments, backbone contributions can significantly alter conformational fluctuations in double-stranded nucleic acid breathing.

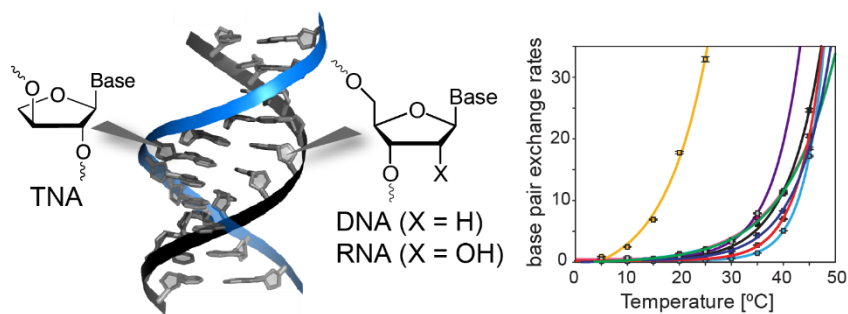
Acknowledgements

This work was supported by the DARPA Fold F(x) Program (N66001-14-2-4054) and National Institutes of Health (GM071461 to ER). We thank Prof. Dr. H. Schwalbe and Dr. H. Steinert for helpful comments on imino proton exchange NMR and Prof. Dr. J. Heemstra for helpful discussions.

Keywords: conformation analysis, DNA, nucleic acid dynamics, RNA evolution, TNA.

- [1] a) K. Schoning, P. Scholz, S. Guntha, X. Wu, R. Krishnamurthy, A. Eschenmoser, *Science* **2000**, *290*, 1347-1351; b) I. Anosova, E. A. Kowal, M. R. Dunn, J. C. Chaput, W. D. Van Horn, M. Egli, *Nucleic Acids Res.* **2016**, *44*, 1007-1021.
- [2] Y. W. Yang, S. Zhang, E. O. McCullum, J. C. Chaput, *J. Mol. Evol.* **2007**, *65*, 289-295.
- [3] L. Orgel, *Science* **2000**, *290*, 1306-1307.
- [4] a) M. O. Ebert, C. Mang, R. Krishnamurthy, A. Eschenmoser, B. Jaun, *J. Am. Chem. Soc.* **2008**, *130*, 15105-15115; b) M. O. Ebert, B. Jaun, *Chem. Biodivers.* **2010**, *7*, 2103-2128.
- [5] C. J. Wilds, Z. Wawrzak, R. Krishnamurthy, A. Eschenmoser, M. Egli, *J. Am. Chem. Soc.* **2002**, *124*, 13716-13721.
- [6] P. S. Pallan, C. J. Wilds, Z. Wawrzak, R. Krishnamurthy, A. Eschenmoser, M. Egli, *Angew. Chem. Int. Ed. Engl.* **2003**, *42*, 5893-5895.
- [7] K.-U. Schöning, P. Scholz, X. Wu, S. Guntha, G. Delgado, R. Krishnamurthy, A. Eschenmoser, *Helv. Chim. Acta* **2002**, *85*, 4111-4153.
- [8] S. P. Sau, N. E. Fahmi, J. Y. Liao, S. Bala, J. C. Chaput, *J. Org. Chem.* **2016**.
- [9] K. Wuethrich, *NMR of Proteins and Nucleic Acids*, John Wiley & Sons, Inc., United States of America, Canada, **1986**.
- [10] J. Cavanagh, W. J. Fairbrother, A. G. Plamer III, M. Rance, N. Skelton, *Protein NMR Spectroscopy. Principles and Practice.*, Elsevier, Academic Press, Amsterdam, Boston, Heidelberg, London, New York, Oxford, Paris, San Diego, San Francisco, Singapore, Sydney, Tokyo, **2007**.
- [11] M. Gueron, J. L. Leroy, *Methods Enzymol.* **1995**, *261*, 383-413.
- [12] M. W. Szulik, M. Voehler, M. P. Stone, *Curr. Protoc. Nucleic Acid Chem.* **2014**, *59*, 7 20 21-27 20 18.
- [13] a) R. Boelens, R. M. Scheek, K. Dijkstra, R. Kaptein, *J. Magn. Reson.* **1985**, *62*, 378-386; b) B. Furtig, C. Richter, J. Wohnert, H. Schwalbe, *ChemBioChem* **2003**, *4*, 936-962.
- [14] a) J. Rinnenthal, B. Klinkert, F. Narberhaus, H. Schwalbe, *Nucleic Acids Res.* **2010**, *38*, 3834-3847; b) H. S. Steinert, J. Rinnenthal, H. Schwalbe, *Biophys. J.* **2012**, *102*, 2564-2574; c) D. Wagner, J. Rinnenthal, F. Narberhaus, H. Schwalbe, *Nucleic Acids Res.* **2015**, *43*, 5572-5585.
- [15] a) C. Chen, I. M. Russu, *Biophys. J.* **2004**, *87*, 2545-2551; b) Y. Huang, X. Weng, I. M. Russu, *Biochemistry* **2011**, *50*, 1857-1863; c) E. Folta-Stogniew, I. M. Russu, *Biochemistry* **1994**, *33*, 11016-11024; d) J. G. Moe, I. M. Russu, *Biochemistry* **1992**, *31*, 8421-8428.
- [16] aH. Lis, N. Sharon, *Chem. Rev.* **1998**, *98*, 637-674; bL. Liu, C. Yang, Q. X. Guo, *Biophys. Chem.* **2000**, *84*, 239-251.

COMMUNICATION



*I. Anosova, E.A. Kowal, N.J. Sisco, S. Sau, J. Liao, S. Bala, E. Rozners, M. Egli, J.C. Chaput and W. D. Van Horn**

Page No. – Page No.

Structural Insights into Conformational Differences between DNA/TNA and RNA/TNA Chimeric Duplexes

TNA, a potential evolutionary precursor of RNA, forms stable anti-parallel Watson-Crick heteroduplexes with DNA and RNA. The reason for its preference for RNA base pairing is unknown. A comparative conformation and dynamics analysis of RNA/TNA and DNA/TNA chimeras shows that A-like helical geometry of heteroduplexes, enforced by TNA, induces previously uncharacterized increased asymmetric breathing at the 5'/2' terminus of TNA/DNA and puts DNA at the limits of its conformational adaptability.

Accepted Manuscript